Jianbo Liu*, Xin Xu, Tianjian Zhang, Jingcheng Wang, Ruifang Wang and Qing Xu

Combined effects of low pressure superheated steam drying and vacuum drying on sugar reduction and quality attribute in mango (*Mangifera indica* L.) slices

https://doi.org/10.1515/ijfe-2023-0249
Received October 9, 2023; accepted April 30, 2024;
published online May 21, 2024

Abstract: Consumers paying more attention to physical health has led to an increasing market demand for low-sugar dried fruit products. The quality of products dried via low pressure superheated steam drying (LPSSD) is not only superior to those dried via conventional hot air or vacuum drying (VD), but also has the potential to reduce sugar content. In order to elucidate the mechanism of reducing the sugar of mango slices by LPSSD and obtain low-sugar dried mango slices, the combined effect of LPSSD–VD on mango slices was studied and an evaporation experiment of a sugar solution in a low pressure superheated steam environment was performed. This study revealed that the sugar reduction of mango slices was mainly due to the superheated steam carryover phenomenon in the second half of the constant-temperature stage and the occurrence of Maillard reaction during LPSSD. The quality attributes of mango slices dried using LPSSD–VD was improved compared with LPSSD and VD. As a result, LPSSD–VD could be used to regulate the sugar content in dried fruit and provide a theoretical basis for the production of low-sugar preserved fruits.

Keywords: mango; superheated steam; vacuum hybrid drying; sugar loss; quality attribute

***Corresponding author: Jianbo Liu**, College of Engineering and Technology, Tianjin Agricultural University, 22 Jinjing Road, Xiqing District, Tianjin 300392, P.R. China, E-mail: qingzhoujianbo@126.com
Xin Xu and Tianjian Zhang, College of Engineering and Technology, Tianjin Agricultural University, 22 Jinjing Road, Xiqing District, Tianjin 300392, P.R. China. https://orcid.org/0009-0008-6428-9495 (X. Xu)
Jingcheng Wang, **Ruifang Wang and Qing Xu,** College of Mechanical Engineering, Tianjin Key Laboratory of Integrated Design and On-line Monitoring for Light Industry & Food Machinery and Equipment, Tianjin University of Science and Technology, 1038 South Dagu Road, Hexi District, Tianjin 300222, P.R. China. https://orcid.org/0000-0001-9447-8117 (Q. Xu)

1 Introduction

Mango (*Mangifera indica L.*) is a seasonal flesh stone fruit, widely grown in tropical and subtropical regions [1], which is a healthy and nutritious fruit containing a high amount of nutrients, dietary fiber, bioactive compounds (pro-vitamin A, vitamin C, and phenolic compounds), and minerals (potassium, iron, and calcium) [2]. The strong seasonality and perishability of fresh mango limit their commercialization, storage, and availability out of season [3].

Drying is the oldest and commonly used preservation method used to extend the shelf life of fruits and reduce postharvest loss. For this, various modern drying techniques have been applied to mango drying in recent years, such as hot air-drying, freeze-drying, solar dehydrated, refractance window drying, osmo-dehydrated [4–7]. These studies mainly focused on the drying characteristic and quality attribute to achieve lower energy consumption and higher quality retention. Nowadays, consumers are concerned about their health and the relationship between food consumption and developing chronic diseases [8]. Therefore, they are not only demanding food products with high nutritional and sensory quality, but also food with low sugar content. Mango is a fruit with high sugar content, and the above drying methods cannot effectively reduce the sugar content of dried mangoes while ensuring product quality attribute, which limits its commercialization. That's why a suitable drying method that can reduce the sugar content without compromising the nutritional properties of mango is in great need.

Superheated steam drying (SSD) is an innovative technology, which provides an oxygen free and sterile environment, with a large heat transfer coefficient and negligible mass transfer resistance [9–11]. Mujumdar et al. [12] reviewed the application of SSD in harvested bio-origin product and found that superheated steam dried products yield better quality attributes than conventional hot air and vacuum drying. Liu et al. [13] reported that the salt content was reduced about 21.5–34.8 % after dried with superheated steam and the protein content in dried soy sauce residue did not change significantly as compared to the original. Wang

et al. [14] found that pineapples dried by superheated steam showed a lower sugar content and superior quality attributes compared to vacuum drying. Therefore, SSD might be an effective method for the production of dried low-sugar fruits such as mango. For SSD at atmospheric pressure, it has a high temperature and is usually used to process grains and its product to improve sensory properties. Schoeman et al. [15] reported that oven roasting had a more adverse effect compared to superheated steam roasting on the physicochemical, structural and functional properties of the flour. Brar et al. [16] compared the hot air and superheated steam treatment on the functional and nutritional properties of yellow pea kernels and found that superheated steam was a much superior alternative to hot air processing as it improved the functional properties without compromising the nutritional properties of yellow peas. Zhong et al. [17] also found that superheated steam stabilization treatment granted cooked black rice the slowest starch digestibility and the highest level of bioaccessible phenolic compounds. Besides, superheated steam had a good effect on the inactivation of spores and salmonella in food [18].

Generally, SSD at atmospheric is unfavorable to dry heat sensitive material such as fruits as its high temperature. To overcome the problem, LPSSD has been applied at a reduced temperature to yield products with minimal loss of nutrients, good hydration capacity, and better color appearance, whose drying pressure is lower than atmospheric pressure [19–21]. Unlike conventional drying, LPSSD has a distinct phenomenon called initial condensation that occurs in the warming up period of drying, transferring an amount of latent heat to the material, which may greatly influence the dried material quality [22]. LPSSD also performs a longer constant-temperature stage on sample surface in the early stage of drying, and the surface temperature of sample dried by the low pressure superheated steam is always higher than that dried by vacuum during the whole drying process. It is important to take into account the special heat and mass transfer properties of superheated steam when drying fruits with LPSSD. Thus far, the application of LPSSD on mango has not reported. Especially, the effect of initial steam condensation period and the superheated steam (as a drying medium) on the sugar loss in fruit during LPSSD is not clear. Additional studies are required to supplement knowledge in this area. Besides, considering the fact that LPSSD is advantageous in performing a longer constant-temperature drying stage and vacuum drying (VD) is performed to maintain a lower sample surface temperature. It might be a good idea to apply VD to preheat the samples followed by LPSSD to prolong the constant-temperature drying stage and improve drying efficiency, and then followed by VD to avoid the deterioration of product quality caused by the high temperature of LPSSD at the final stage. Also, it is possible to regulate the sugar content in dried mangoes products by setting the inlet time of superheated steam. That is why we are supposed to propose a hybrid drying method for mango based on the coupling of sugar content and quality attribute.

Understanding the sugar loss mechanism of mango during LPSSD is the basis for producing low-sugar and high-quality dried mango. Therefore, the objectives of this paper were to (1) study the influence of steam condensation occurred in mango surface and superheated steam (as a drying medium) on sugar loss, clarifying the sugar loss mechanism in mango during LPSSD; (2) evaluate drying characteristics, sugar ratio and quality attribute in terms of color, vitamin C content and microstructure under the hybrid drying method namely VD-LPSSD.

2 Materials and methods

2.1 Materials

The mango slices cultivar, Tainong No. 1 that was produced in Guangdong Province, China, with a w.b. of 70–80 %, was used as the experimental material. The mango slices weighed 500–700 g each and were free of disease and pests. Before each experiment, fresh mango slices were cleaned, peeled, and cut into 4 ± 0.5 mm thin slices. Due to the absence of oxygen in the LPSSD, oxidation reaction does not occur during the drying of mango slices. Therefore, Vitamin C (VC) reagent was not added to the fresh samples for antioxidant pretreatment. The initial dry-basis moisture content of fresh mango slices was 5.54 ± 0.43 kg kg^{-1} (d.b.). According to the industry standard NY/T 1041-2018, the moisture content of dried mango slices for safe storage was less than 20 g/100 g. The drying process was considered complete when the dry-basis moisture content of mango slices reached about 0.176 kg kg^{-1}(d.b.).

2.2 Sugar solution

A sugar solution was selected as an experimental simulation material to simulate the sugar solution on the surface of mango slices during the drying process and served as a control. The composition of the model sugar solution is fructose. In order to study the effect of operating pressure on the loss of sugar in the sugar solution, a sugar solution with a concentration of 0.1 mg mL^{-1} was prepared and the low pressure superheated steam test was carried out at 9, 11 and 13 kPa under the heating temperature of 85 °C. To reveal the effect of heating temperature on sugar reduction of sugar solution, a sugar solution with a concentration of 0.1 mg mL^{-1} was prepared and tested at 80, 85 and 90 °C respectively. To study the effect of sugar concentration on sugar reduction in sugar solution, sugar solution at concentrations of 0.1, 1 and 5 mg mL^{-1} was prepared and tested at a pressure of 9 kPa and 90 °C. Each set of experiments was performed for 4 h, all experiments were repeated three times, and the results were expressed as arithmetic mean ± standard deviation.

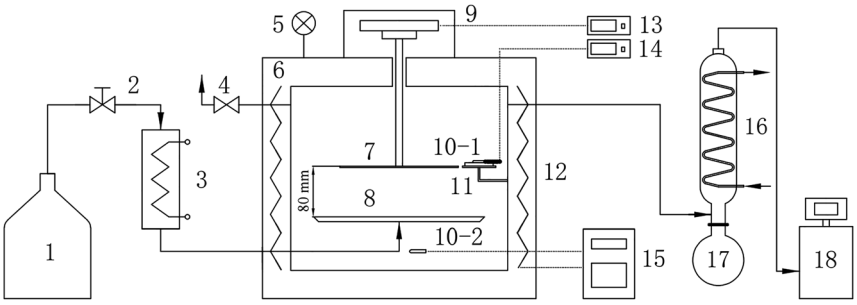


Figure 1: Schematic diagram of low-pressure superheated steam drying device. (1) Steam generator. (2) Regulating valve. (3) Steam heating device. (4) Steam pressure regulating valve. (5) Vacuum meter. (6) Heating plate. (7) Material pallets. (8) Steam distributor. (9) Weight detection device. (10-1) Material temperature detection device. (10-2) Steam temperature detection device. (11) Control sample tray. (12) Drying chamber. (13) Weight acquisition device. (14) Temperature acquisition device. (15) Control panel. (16) Condensation unit. (17) Condensate collection device. (18) Diaphragm vacuum pump.

2.3 Experimental setup

The LPSSD device used in this experiment was shown in Figure 1. The complete apparatus was composed of a steam generator, steam superheater, vacuum drying chamber, condensing system, vacuum pump (BUCHI V-710, Labortechnik AG, Switzerland), and an online data acquisition system (G&G, Changzhou, China). The inner chamber (12) was 300 mm × 300 mm × 275 mm. An electric heater was placed between the layers of the inner and outer chambers. The steam distributor (8) contained holes of 3 mm diameter and an opening rate of 2.5 %. The material tray (7) was made of polyfluorotetraethylene, which had many small holes to facilitate full contact between the material and the steam. The material tray was connected to a weight detector (G&G, Changzhou, China) and can display the material weight online. The thermocouple, of the material temperature detection device, measured the temperature of the control sample material in the drying chamber in real-time. The inner and the outer layer of the chamber were lined with thermal insulation materials to reduce heat loss.

For LPSSD, the drying chamber is first heated to the desired temperature, and then the mango slices or sugar solution control are quickly placed into the drying chamber to guarantee that the stable temperature of the drying chamber will not be disrupted. Then the vacuum pump starts to work, and after about 100 s, the drying chamber will reach the required vacuum level. When the drying chamber reaches the target vacuum level, superheated steam is introduced. Due to the small flow of superheated steam and the high control accuracy of the vacuum pump, the vacuum stability of the drying chamber is not affected. For VD, the drying chamber is first heated to the set temperature, and then the experimental material is quickly placed into the drying chamber to avoid the destruction of the drying chamber stable temperature. The vacuum pump is then turned on to stabilize the pressure of drying chamber at the target vacuum level. Due to the high control accuracy of the vacuum pump, LPSSD and VD can be switched directly without affecting the vacuum level of the drying chamber.

2.4 Relative moisture content (MR)

The dry-basis mass of the sample, determined according to AOAC 925.10 (2002) [23] was expressed as:

$$M_t = \frac{(m_t - m_g)}{m_g} \tag{1}$$

where M_t was the dry-basis moisture content of mango slices at time t, kg kg^{-1} (d.b.). m_g was the absolute dry mass of the mango slices (g). m_t was the mass of the mango slices at time t (g).

The dry-basis moisture content of fresh mango slices was 5.54 ± 0.43 kg kg^{-1} (d.b.). Considering that the initial dry-base moisture content was different for each mango slices, the moisture relative content (MR) was used to describe moisture content during the drying process. MR indicated the ratio of the dry-basis moisture content of the material to the initial dry-basis moisture content at time t. MR was expressed as:

$$\mathrm{MR} = \frac{(M_t - M_e)}{(M_t - M_o)} \tag{2}$$

where M_e was the equilibrium moisture content, kg kg^{-1}(d.b.). M_o and M_t were the initial moisture content of the mango slices and moisture content at time t, kg kg^{-1} (d.b.), respectively.

2.5 Drying rate

Drying rate (N) refers to the mass of moisture removed per unit time per g dry mass of mango slices [24].

$$N = \frac{\Delta m}{\Delta t \times m_g} \tag{3}$$

where N was the drying rate of mango slices at time t kg kg^{-1} (d.b.) min^{-1}. m_g was the absolute dry mass of mango slices (g), Δm was the removed moisture mass in Δt (g), and t was the drying time (min).

2.6 Sugar ratio

The sugar content in fresh mango slices and dried products was determined through colorimetric method using 3,5-dinitrosalicylic acid (DNS) [25]. The sugar content was determined according to NY/T 242-2015. The standard curve equation was obtained by correlating the glucose concentration with its corresponding peak area, as follows:

$$y_1 = 11.14562x_1 \left(R^2 = 0.9924\right) \tag{4}$$

where y_1 was the glucose concentration (mg L^{-1}) and x_1 was the absorbance of glucose.

Sugar ratio was used to express the change in sugar content between dried and fresh mango slices.

$$S = s_t / s_o \tag{5}$$

where S was the sugar ratio at drying time t. S_t was the sugar mass in mango slices at drying time t (g). S_o was the initial sugar mass in the mango slices (g).

2.7 Detection of vitamin C

Agilent 1200 high performance liquid chromatography (HPLC, Agilent, California State, America) was used to qualitatively and quantitatively analyze the VC content in mango slices [26]. HPLC, for VC measurement, was performed using with an Eclipse XDB C-18 column (4.60 mm × 150 mm, 5 μm, Agilent, California State, America). The detection wavelength, column temperature, and sample volume was 254 nm, 25 °C, and 10 μL per injection, respectively.

The standard curve equation was given as:

$$y_2 = 23.36457x_2 + 2339.6 \left(R^2 = 0.996\right) \tag{6}$$

where y_2 was the peak area of VC detected using HPLC and x_2 was the VC concentration (mg L^{-1}). VC detected using liquid chromatography and VC concentration exhibited a positive linear correlation (R^2 = 0.996), within the concentration range of 25–150 mg L^{-1}. The VC content of fresh mango slices was measured to be 99.58 mg·100 g^{-1}.

2.8 Color

A handheld spectrophotometer (NS 800, Sanenchi Technology Co., Ltd. Shenzhen, China) was used to detect the color change of mango slices before and after drying [27]. Five pieces of the material were selected for each experiment, and their color was measured six times, along several points on the mango slices. The arithmetic mean of the 30 measurements was calculated. L^*, a^*, b^* indicated the colors of the materials [28]. L^* value, ranging from 0 to 100 (black to white), represented the brightness value of the mango slices. a^* value, ranging from −60 to 60, represented the red or green value of mango slices. b^* value, ranging from −60 to 60, represented the yellow or blue value of mango slices. The change in the total color difference could be expressed using the following formula [29]:

$$\Delta E = \sqrt{(\Delta L^*)^2 + (\Delta a^*)^2 + (\Delta b^*)^2} \tag{7}$$
$$\Delta L^* = L^* - L_0^* \quad \Delta a^* = a^* - a_0^* \quad \Delta b^* = b^* - b_0^*$$

where ΔE^* value was the change in the total color difference between the fresh and dried mango slices. ΔL^* value was the brightness difference between fresh and dried mango slices. Δa^* value was the change in red or green values between the fresh and dried mango slices. Δb^* value represented the change in yellow or blue values between the fresh and dried mango slices.

2.9 Microstructure

The internal structure of the dried mango slices was observed using a Zeiss Sigma 300 scanning electron microscopy (Carl Zeiss AG, Germany) [30], at a magnification of 500×. Each sample was photographed thrice at different locations. Before testing, each sample was sprayed with gold and then a specialized conductive adhesive was used to fix the sample on the SEM testing platform. 1–18 groups of samples could be tested each time.

2.10 Low pressure superheated steam drying combined vacuum drying (LPSSD–VD)

For LPSSD, it has a distinct property, i.e., there is an inversion temperature. When the drying temperature is above the inversion temperature, the drying rate of LPSSD is higher than that of VD, and when the drying temperature is below the inversion temperature, the drying rate of LPSSD is lower than that of VD [31]. Considering the drying rate and quality attributes, 80 °C, 85 °C and 90 °C were selected as the drying temperature, which was near the inversion temperature. VD was performed at the beginning stage of the constant-temperature drying stage to maintain a low internal temperature of the mango slices. LPSSD was performed at the later stage of constant-temperature drying to prolong the constant-temperature drying stage and improve drying efficiency. However, it could promote the migration and loss of sugars. VD was used in the second stage of drying, to avoid the deterioration of product quality caused by the high temperature of LPSSD, until the mango slices reached the target moisture content. The specification of LPSSD–VD was as follows: at drying temperature of 90 °C: VD was performed for 0–40 min, LPSSD for 40–100 min, followed by vacuum drying until the process was complete; at a medium temperature of 85 °C: VD was performed for 0–100 min, LPSSD for 100–160 min, followed by VD until the process completes. The operating pressure was maintained at 9 kPa.

2.11 Statistical analysis

Origin 2022 (OriginLab Corp., Northampton, MA, USA) software was used to graph the results. SPSS Statistics (version 27.0, IBM Corp., Armonk, NY, USA) was used for data analysis. Duncan's multiple tests were used for one-way ANOVA. The significant difference between the data was considered if the p-value was less than 0.05.

3 Result and discussion

3.1 Internal temperature change of mango slices

The internal temperature changes in the mango slices during LPSSD and VD were shown in Figure 2. For the LPSSD and VD, the entire drying process could be divided into three stages: stage I, the heating stage; stage II, the constant-temperature stage; and stage III, the second heating stage. In stage I, the temperature of the material raise rapidly and stabilized at the water evaporation temperature on the mango slices surface. In stage II, for VD, the internal temperature of mango slices was always maintained at the wet-bulb temperature during the constant-temperature stage, which was higher than LPSSD. The similar result was reported by Wang et al [32]. For LPSSD, the internal temperature of the mango slices should theoretically be equal to the boiling point temperature at the operating pressure. The water boiling point temperature of

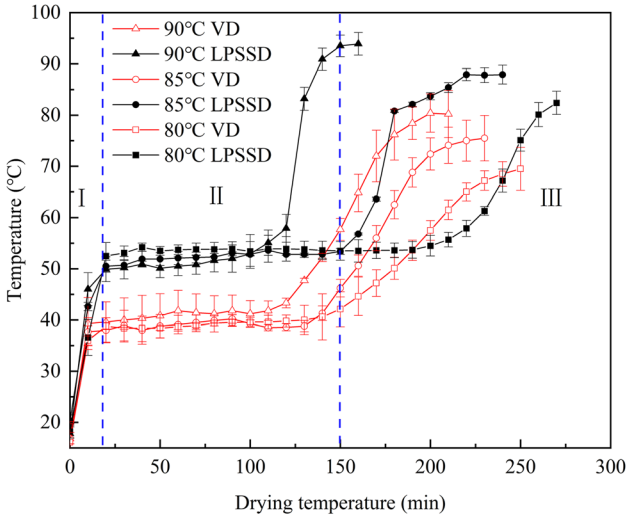


Figure 2: Temperature of mango slices dried using different drying methods.

was 45 °C when the drying pressure was 9 kPa. However, the internal temperature of the mango slices in this study was 53 °C, which was higher than 45 °C. This was due to the fact that a heating coil was installed in the experimental setup in order to avoid condensation, and the mango slices internal temperature was higher than the boiling point temperature when other heat transfer methods were present. The LPSSD had a shorter secondary heating stage than VD (Figure 2), which was consistent with Devahastin et al. [33] and Liu et al [34]. Additionally, the temperature difference between the medium and mango slices surface increased, which promoted the drying rate, and the overall drying time and constant temperature period time decreased with an increase in the drying temperature for both VD and LPSSD (Figure 2), which was also obtained by Sittiritkawin et al. [35] who reported that the influence of the LPSSD on pumpkin under different drying pressures and temperatures. This was due to the increase in medium temperature results in an increase in the external diffusion rate of moisture on the mango slices surface. In addition, the dynamic balance of moisture inside and on the surface of mango slices surface was disrupted faster. This shortened the constant-temperature stage. Nimmol et al. [36] also found a longer constant-temperature stage at a lower temperature during the LPSSD of banana slices.

3.2 Effect of low pressure superheated steam on sugar ratio of the sugar solution

Figure 3(a) and Figure 3(b) displayed the change in sugar ratio of the sugar solution (control) at different heating temperatures and pressures, respectively, under a low-pressure superheated steam environment. Sugars were detected in the condensate at different drying temperatures. When the sugar solution was heated in a vacuum environment, the presence of sugar was hardly detected in the condensate. This was consistent with the result of Matsuura et al. [37] who reported that 12.8 % salt was removed from chicken meat using superheated steam drying, whereas only 0.2 % salt was removed with hot air drying at the same drying time. Liu et al. [13] also found that the salt reduction in soy sauce residue was due to the salt precipitation caused by condensate appearing on the soy sauce surface during superheated steam drying. The studied demonstrated that not only condensate could reduce the composition of the experimental materials, but also superheated steam as a drying medium could cause the migration of sugar from the solution, which was defined as superheated steam carryover phenomenon. The sugar ratio of the sugar solution and condensate were significantly different (p<0.05) at different

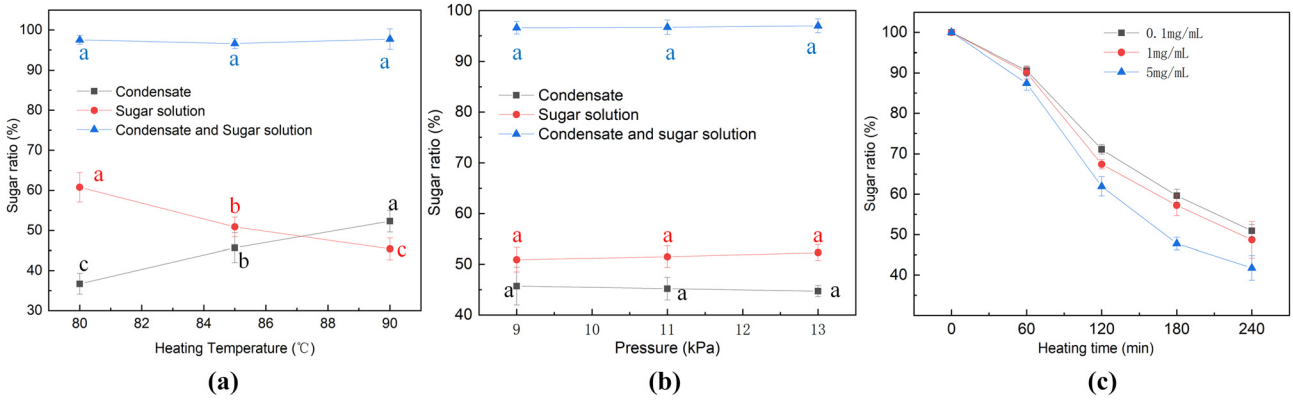


Figure 3: Change in the sugar ratio (%) of sugar solution under low pressure superheated steam with different heating temperatures (a), pressure (b), and heating time (c).

heating temperature, but sugar ratio of the sugar solution and condensate were not significantly different (p>0.05) at different pressure. The heating temperature had a greater effect than the pressure on sugar migration. Additionally, the sum of the amount of sugar recovered in the condensate and that retained in the sugar solution were not significantly different (p>0.05) at different temperature and pressure, which accounts for 96.6–97.7 % of the initial sugar solution under different operating conditions. Therefore, the sugar loss was negligible. This could be attributed to the lack of amino compound required for the Maillard reaction in sugar solutions and the Maillard reaction did not occur. The sugar only migrated with the superheated steam and did not decompose via the carbonyl-ammonia reaction.

Figure 3(c) showed the variation in the sugar ratio in a low-pressure superheated steam environment with varying sugar solution concentrations. As shown in Figure 3(c), the sugar ratio of the sugar solution decreased with an increase in concentration when heated for the same time. It illustrated that more sugar was in contact with the superheated steam on the surface of sugar solution and more sugar was carried out due to the superheated steam carryover phenomenon with the increase of concentration of the sugar solution. It was further indicated that superheated steam, as a drying medium, could promote the loss of sugar in mango slices.

3.3 Change of sugar ratio in mango slices during LPSSD–VD

Figure 4(a) showed the change in the sugar ratio of mango slices and its condensate during the LPSSD at different drying temperatures. The sugar ratios of dried mango and condensate were both significantly different (p>0.05) at different temperature. The sum of the sugar ratios in the condensate and mango slices was significantly lower than that in the sugar solution control. This showed that sugar migrated to the condensate and reacted with the amino acids in mango slices at high temperatures, which resulted in a greater sugar loss. Additionally, the sum of the sugar ratios in the condensate and mango slices were not significantly different (p>0.05) at 80 °C and 85 °C. The most sugar ratio (45.67 %) was retained at a moderate drying temperature of 85 °C. This was consistent with Suvarnakuta et al. [38] who found that the maximum retention of α-mangostin and 8-desoxygartanin was obtained at a moderate drying temperature of 75 °C when the mangosteen rind was dried by LPPSD at 60 °C, 75 °C and 90 °C respectively. The degradation of sugar was affected by many factors, such as drying time, the presence of oxygen, and drying temperature et al [14]. At 90 °C, although the drying time was reduced, the material temperature was higher, which intensified the Maillard reaction, thereby accelerating the decomposition of sugars. At 80 °C, although the Maillard reaction was slow due to the decrease of temperature, the reaction was prolonged because of the increase in the drying time, thus, promoting the decomposition of sugar. It could be seen from Figure 4(b) that the sugar ratios of condensate were not significantly different (p>0.05) at different operating pressure, but the sugar ratios of dried mango at 11 kPa and 13 kPa were significantly different (p<0.05) with that at 9 kPa. Operating pressure had a limited effect on the sugar content comparted to drying temperature.

Figure 5 and Figure 6 showed the sugar ratio in dried mango slices and condensate, for LPSSD and VD, when the drying pressure was 9 kPa and drying temperature was 85 °C

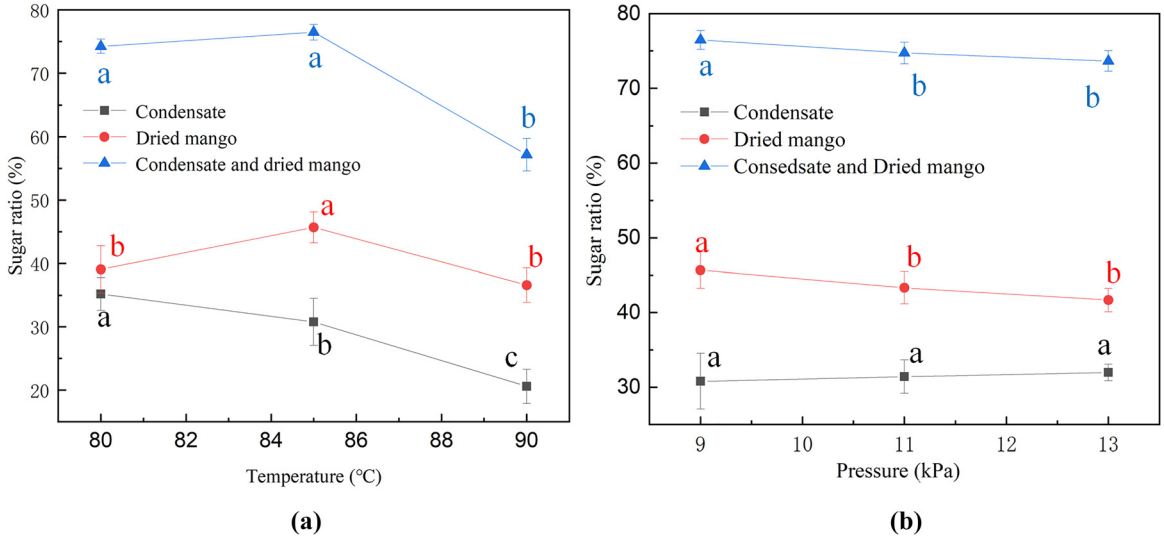


Figure 4: Sugar ratio (%) of mango dried using LPSSD at different drying temperatures (a) and pressure (b).

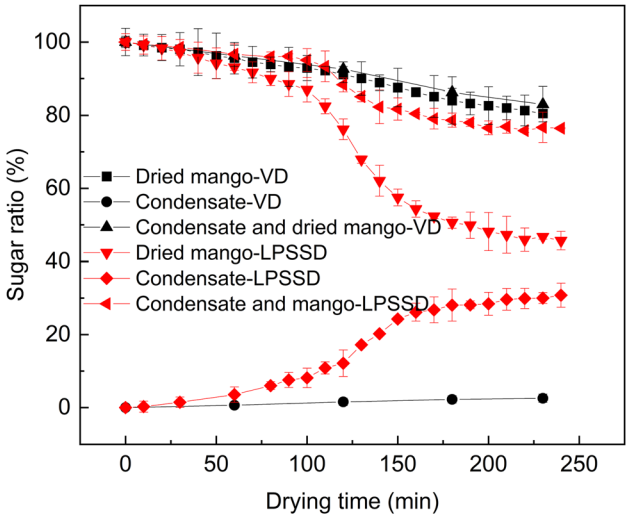


Figure 5: Sugar ratio of mango slices at different drying times (min) with drying methods (85 °C, 9 kPa).

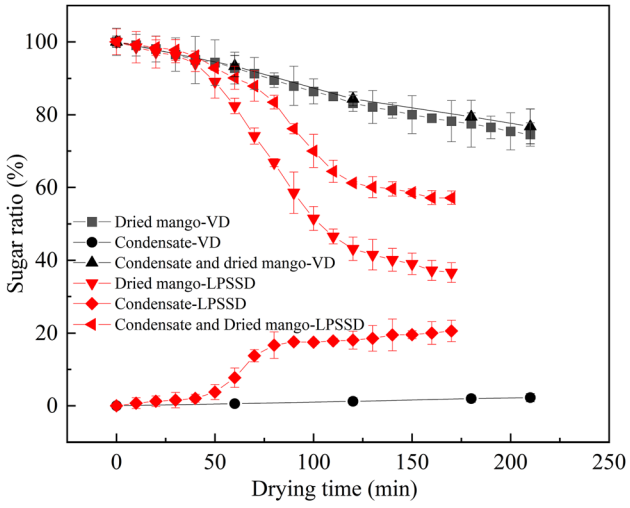


Figure 6: Sugar ratio of mango slices dried using different drying methods (90 °C, 9 kPa).

and 90 °C, respectively. The final sugar ratio of mango slices dried using LPSSD was lower than that dried using VD. This was because the internal temperature of mango slices for LPSSD was higher than that for VD in the constant-temperature stage, which intensified the Maillard reaction, thereby resulting in a greater sugar reduction. In addition, the superheated steam carried more sugar into the condensate, which was one of the main factors for sugar reduction in mango slices during LPSSD. This was consistent with the results of Liu et al. [39] who found that a large amount of vitamin C entered the condensate during the LPSSD of green turnip.

Furthermore, the sugar migration caused by superheated steam carryover phenomenon was mainly concentrated in the second half of the constant-temperature stage: the 100–160 min stage when drying at 85 °C and 40–100 min stage at 90 °C. This might be the sugar concentration on mango slices surface was low during the early stage of drying, and the superheated steam carryover phenomenon was weak. As the drying process progressed, more water evaporated and the concentration of the surface sugar solution increased, which resulted in superheated steam carryover phenomenon intensified. As a result, more sugar migrated into the condensate. In the later stage of drying, it was difficult for the moisture inside the mango slices migrated to the surface, and the surface moisture decreased, which slowed down the superheated steam carryover phenomenon. By comparing the sugar reduction characteristics during LPSSD and VD of mango slices, it was determined that the superheated steam carryover phenomenon was mainly concentrated in the later period of the constant-temperature stage. According to this principle, a combination of LPSSD and VD could effectively control the sugar content of mango slices during the drying process.

3.4 Combination of LPSSD and VD

3.4.1 Drying kinetics

The internal temperature change of the mango slices during LPSSD–VD was shown in Figure 7. For 85 °C, the ending temperature of mango slices under LPSSD–VD was 81.4 °C, which was 6.9 °C lower than that of LPSSD and 5.5 °C higher than that of VD (Figure 7(a)). The drying time under LPSSD–VD reduced by compared with 16.6 % and 13.1 % compared to LPSSD and VD, respectively. For 90 °C, the ending temperature of mango slices under LPSSD–VD was 88.1 °C, which was 5.8 °C lower than that of LPSSD and 7.9 °C higher than that of VD (Figure 7(b)). The drying time under LPSSD–VD reduced by 6.3 % and 28.6 % compared to LPSSD and VD, respectively. With the increase of drying temperature, the time of LPSSD–VD decreased significantly, which was due to the presence of inversion temperature during LPSSD. The rate of LPSSD was higher than that of VD and when the drying temperature was higher than the inversion temperature [31].

VD was adopted in the early stage of LPSSD–VD (Figure 8) to avoided steam condensation, and the drying rate did not show a negative value [40]. The drying rate increased compared to VD when the LPSSD stage was added. This showed that LPSSD–VD could reduce the surface temperature of mango slices and increase the drying rate.

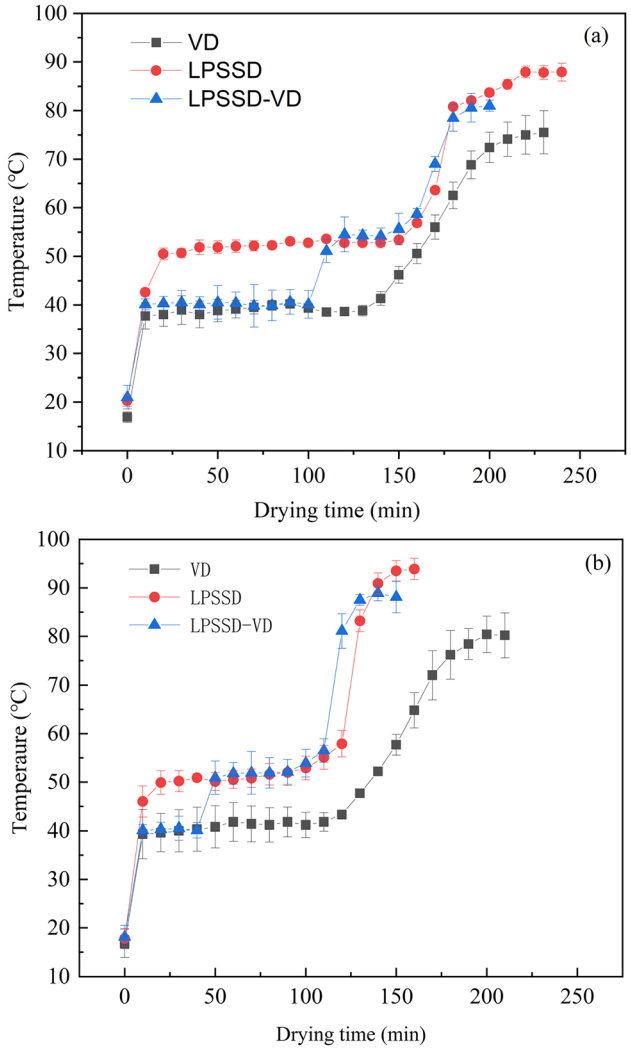


Figure 7: Temperature of mango slices using different drying methods at the drying temperature of 85 °C (a) and 90 °C (b).

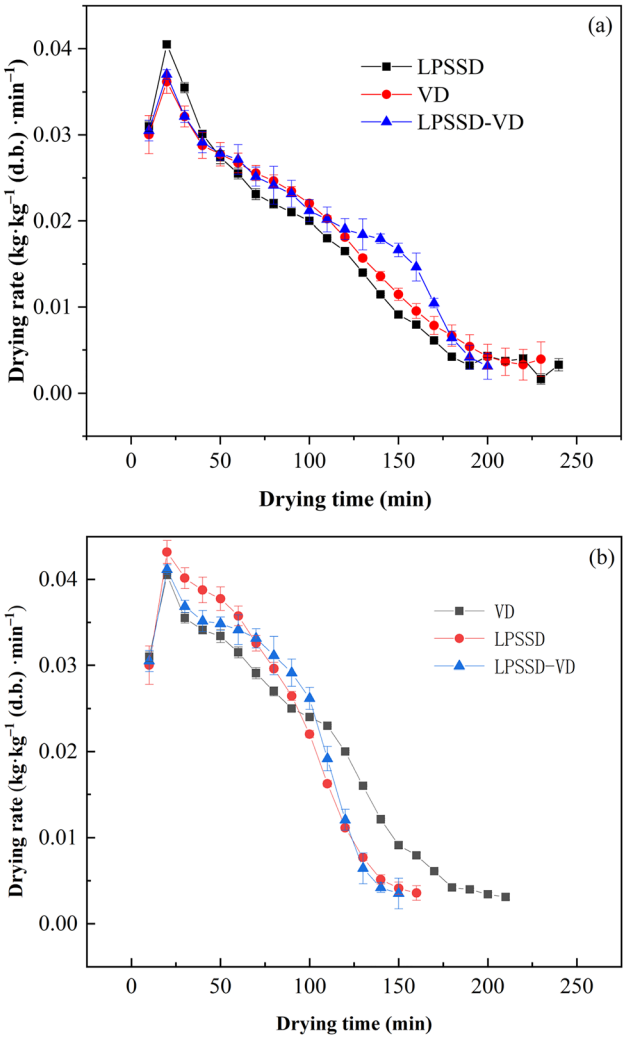


Figure 8: Drying rate of mango slices using different drying methods at the drying temperature of 85 °C (a) and 90 °C (b).

3.4.2 Microstructure

The longitudinal cross-sectional microstructures of mango slices dried using LPSSD and VD, and LPSSD–VD at 90 °C and 85 °C were shown in Figure 9 and Figure 10, respectively. The cross-section of mango slices dried at different drying conditions presented pore structures with different sizes and densities. The number of pores and pore sizes of mango slices dried via LPSSD–VD were increased compared to those dried by VD and LPSSD. The pore structure of green and white radish dried by LPSSD was also better than that of VD. The greater number of pore structures was more convenient for the diffusion of internal moisture and improved the drying rate in the late drying stage. This was one of the reasons why LPSSD–VD could reduce the drying time. The surface of mango slices, dried via LPSSD–VD, did not exhibit hardening or crusting due to the surfaces of samples were always in a moist vapor environment [12]. The internal moisture could better migrate from the inside of the mango slices to the surface, thereby slowing down the damage caused by internal stress to the internal texture of the mango slices. Numerous honeycomb structures formed inside the mango slices, which could absorb more free water during the rehydration process, thus, facilitating better rehydration performance [41].

3.4.3 Sugar ratio

The sugar ratio of mango slices dried at 85 °C and 90 °C using LPSSD, VD, and LPSSD–VD were shown in Figure 11. The sugar ratio of mango slices were significantly different (p<0.05) for different drying methods at 85 °C and 90 °C. For 85 °C, the sugar ratio of mango slices dried using LPSSD–VD

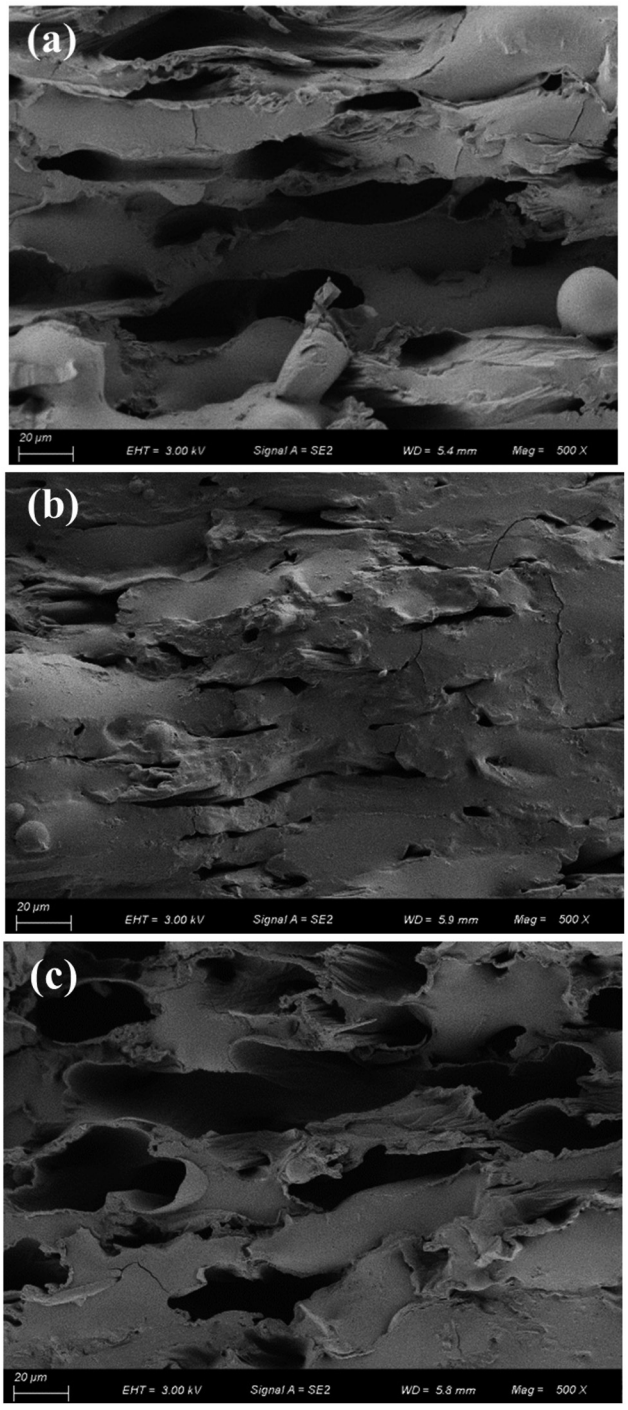


Figure 9: Micro-structure of mango slices dried using different drying methods at the drying temperature of 85 °C. (a) LPSSD (b) VD (c) LPSSD–VD.

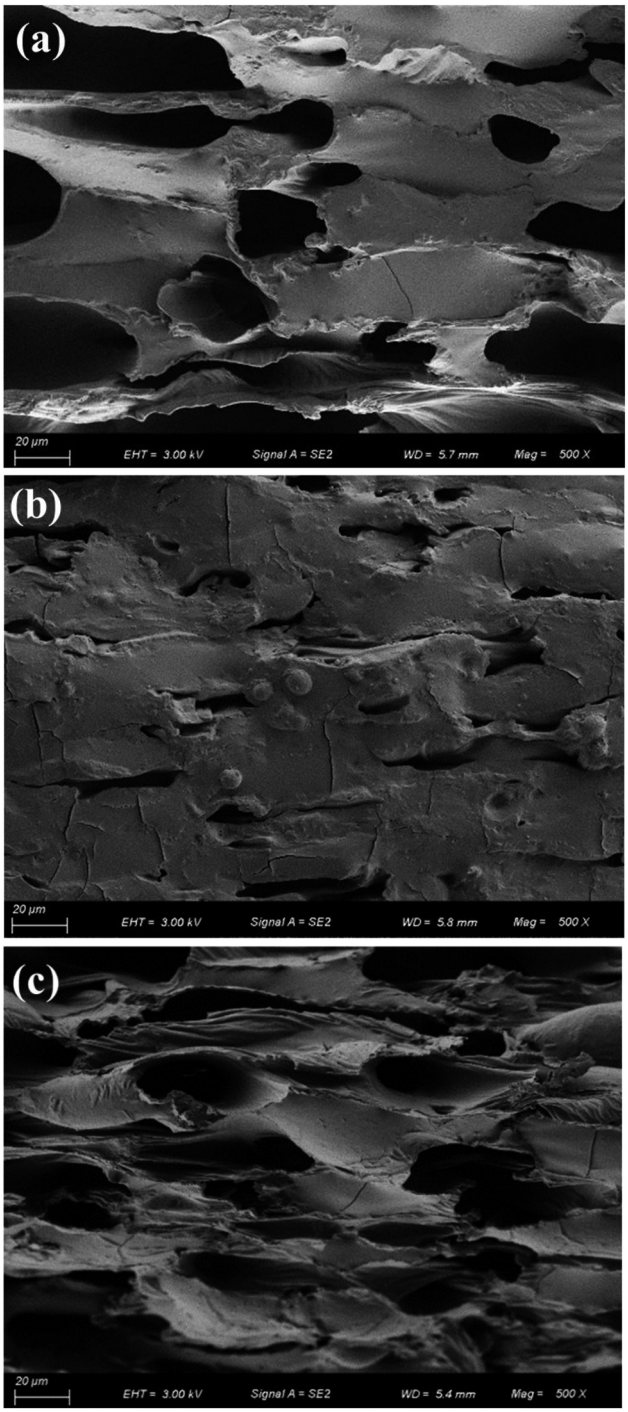


Figure 10: Micro-structure of mango slices dried using different drying methods at the drying temperature of 90 °C. (a) LPSSD (b) VD (c) LPSSD–VD.

was 59.64 %, which was 130.6 % and 74.1 % of that dried using LPSSD and VD. For 90 °C, the sugar ratio of mango slices dried using LPSSD–VD was 47.64 %, which was 130.2 % and 63.9 % of that dried using LPSSD and VD. The result was consistent with Wang et al. [14] who found that the sugar content of dried bananas dried by LPSSD was between LPSSD and VD. The introduction of superheated steam coincided with the main stage of sugar reduction, where the sugar on the mango slices surface came into contact with the superheated steam to produce a strong superheated steam

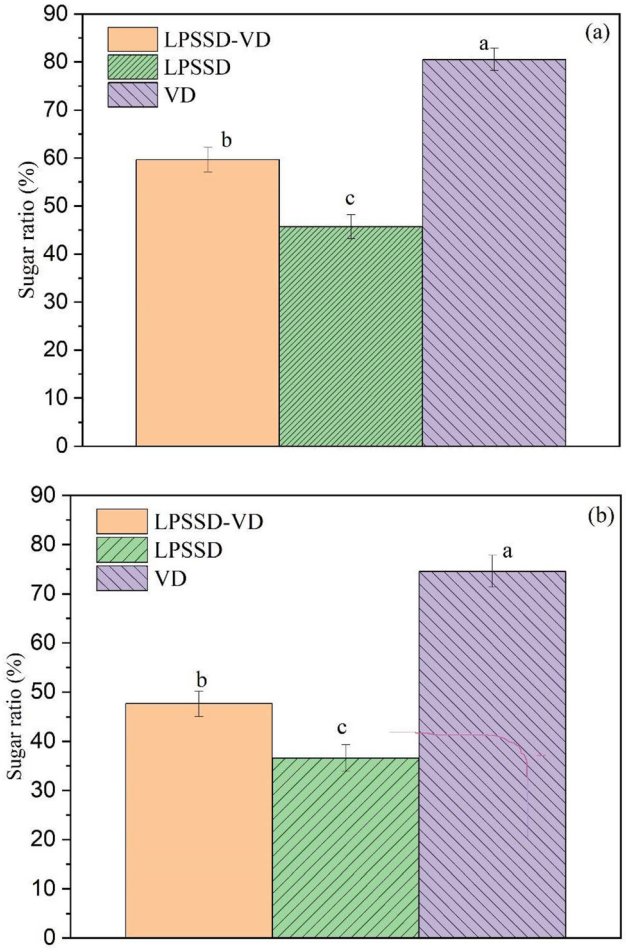


Figure 11: Sugar content of dried mango slices using different drying methods at a drying temperature of 85 °C (a) and 90 °C (b).

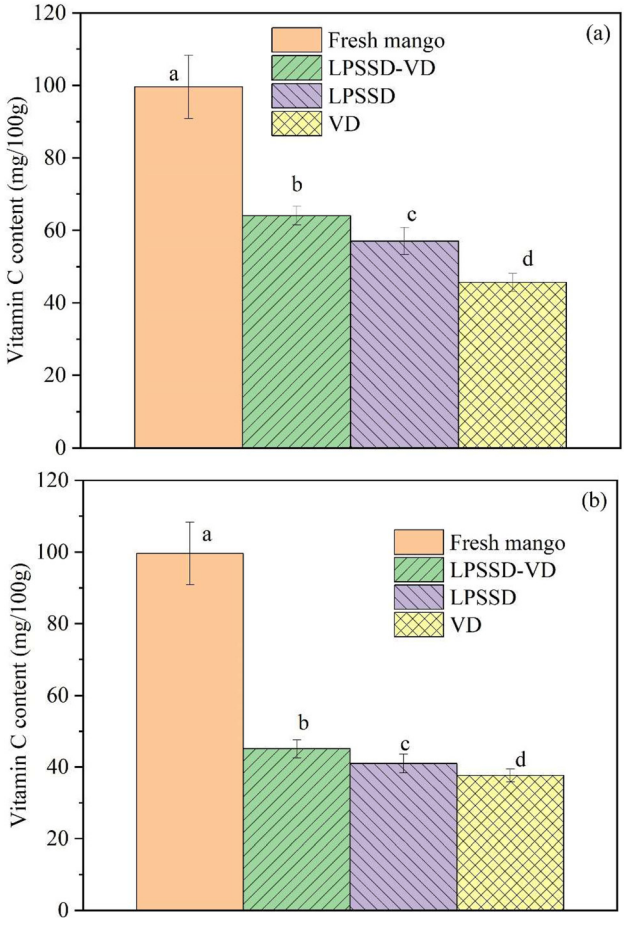


Figure 12: VC content of mango slices using different drying methods at the drying temperature of 85 °C (a) and 90 °C (b).

carryover phenomenon. The amount of sugar reduction could be adjusted by adjusting the superheated steam introduction time to control the sugar content in dried mango slices at a desired level. As a result, the product could meet the health requirements of low sugar content while ensuring a satisfactory taste.

3.4.4 Vitamin C (VC) content

Vitamin C was one of the most commonly measured nutrients for assessing nutrient loss during drying [42]. The VC retention of mango slices dried using LPSSD, VD, and LPSSD–VD at 90 °C and 85 °C was shown in Figure 12. It showed that there was significant difference (p<0.05) in the VC of the mango slices for different drying methods. For 85 °C, the VC retention rate of mango slices dried using LPSSD–VD was 64.27 % (64.01 ± 2.55 mg/100 g), which was 112.2 % and 140.2 % of that dried using LPSSD and VD. For 90 °C, the VC retention rate of mango slices dried using LPSSD–VD was 45.3 %, which was 110.1 % and 119.8 % of that dried using LPSSD and VD. The VC retention of the dried pineapple by LPSSD–VD was the highest compared to LPSSD and VD [14]. General, the presence of oxygen and increase in temperature could accelerate the oxidation and degradation of VC [43]. Compared with LPSSD, LPSSD–VD retained a lower constant-temperature (due to VD), which slowed down the degradation of VC. Compared with VD, the introduction of LPSSD reduced the contact time between mango slices and oxygen, which reduced the loss of VC due to the inhibition of the oxidation reaction.

3.4.5 Color

The color of the mango slices dried using LPSSD, VD, and LPSSD–VD were shown in Figure 13. The L^* of the mango slices dried by LPSSD and VD were not significantly different (p>0.05), but the L^* of the dried mango slices were significantly different (p<0.05) from those of the fresh mango slices. Compared with LPSSD and VD, the L^* value of mango slices

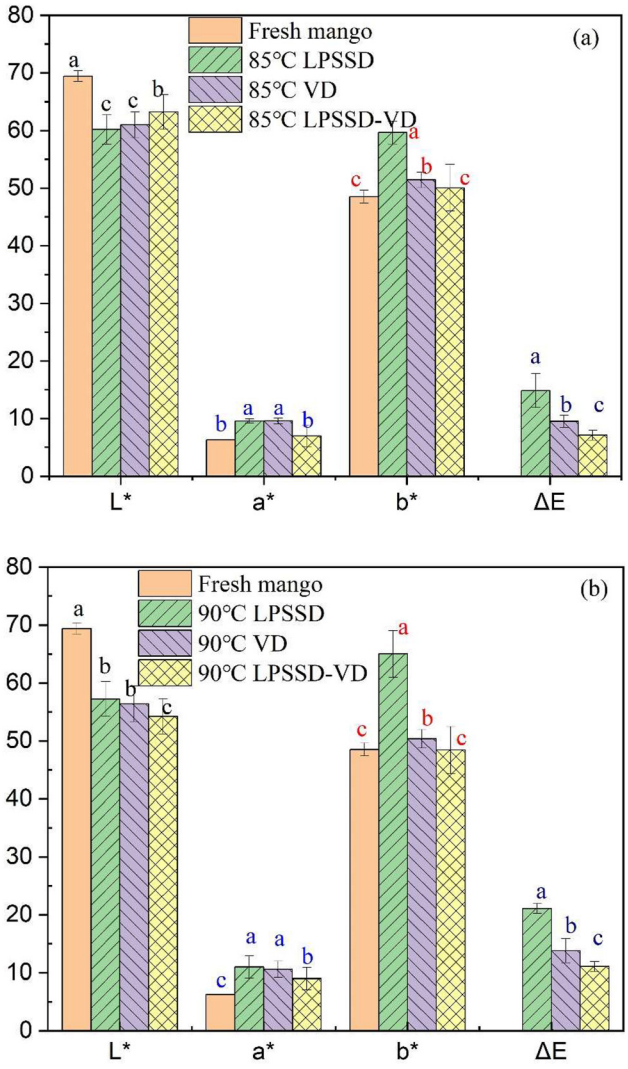


Figure 13: Color measurements of dried mango slices using different drying methods at the drying temperature of 85 °C (a) and 90 °C (b).

dried at 85 °C using LPSSD–VD was closer to that of fresh mango slices than that using LPSSD and VD. Additionally, the L^* value change was smaller than that obtained when the mango slices was dried at 90 °C. The literature reported that increasing the drying temperature resulted in lower L^* value during SSD of banana [44]. There was no significant difference ($p>0.05$) in a^* value between fresh and LPSSD–VD samples at 85 °C, but the a^* value increased significantly ($p<0.05$) at 90 °C. The a^* value of mango slices dried using LPSSD–VD exhibited a downward trend compared with LPSSD and VD. The b^* value of mango slices dried by LPSSD–VD was not significantly different ($p>0.05$) from that of the fresh mango slices, but the b^* value of mango slices dried by LPSSD and VD increased significantly ($p>0.05$). The development of mango slices' a^* and b^* values could be attributed to the enzymatic and non-enzymatic browning during drying [44]. This indicated that the lower constant-temperature of the LPSSD–VD slowed the Maillard reaction. Simultaneously, shortening the overall drying time of LPSSD–VD reduced the time of the Maillard reaction, which in turn reduced the color deterioration of dried mango slices caused by non-enzymatic browning. The ΔE^* value of mango slice dried by different methods was significant difference ($p<0.05$). For 85 °C, the total color difference value ΔE^* value of mango slices dried using LPSSD–VD was 47.7 % and 74.7 % of that dried using LPSSD and VD. For 90 °C, the total color difference value ΔE^* value of mango slices dried using LPSSD–VD was 52.5 % and 80.2 % of that dried using LPSSD and VD. This showed that LPSSD–VD significantly improved the color of the dried mango slices compared to LPSSD and VD. Since LPSSD processing was an oxygen-free process except in the initial stage, the Maillard reaction instead of an enzymatic reaction may be the main reason for the color change [45]. The color changes during LPSSD processing typically occur during the initial stage when LPSSD was condensed on the food surface [46].

4 Conclusions

In this paper, sugar solution was used as a control experiment and the effect of superheated steam as a drying medium on sugar loss was revealed. Then, the combined effect of LPSSD and VD on the sugar reduction and quality change in mango slices were also studied. The main conclusions were as follows:

Superheated steam, as a drying medium, could promote sugar reduction, named as superheated steam carryover phenomenon. The sugar reduction of mango slices was mainly due to the superheated steam carryover phenomenon and occurrence of the Maillard reaction. The reduction of sugar in mango slices caused by superheated steam carryover phenomenon was mainly concentrated in the second half of the constant-temperature stage. LPSSD–VD could be used to regulate the sugar content of dried mango slices. For drying quality, the VC retention rate in mango slices dried by LPSSD–VD was higher compared to LPSSD and VD, which reached a maximum of 64.27 % at 85 °C and 9 kPa. The total color difference value ΔE^* of mango slices dried using LPSSD–VD was smaller than that dried using LPSSD and VD. The pore structure of mango slices dried using LPSSD–VD was also improved compared to LPSSD and VD. In conclusion, LPSSD–VD can be used as an option to yield low-sugar preserved fruits without the reduction of quality attributes.

Research ethics: The local Institutional Review Board deemed the study exempt from review.

Author contributions: The authors have accepted responsibility for the entire content of this manuscript and approved its submission.

Competing interests: The authors states no conflict of interest.

Research funding: The authors express their appreciation to Tianjin Science and Technology Project under the contract no. 22ZYCGSN00660, Tianjin Science and Technology Project under the contract no. 23YDTPJC00630 and Scientific Research Projects of Tianjin Municipal Education Commission under contract no. 2023ZD002.

Data availability: Not applicable.

References

1. Yitayew T, Fenta T. The effect of drying method on the texture, colour, vitamin C and β-carotene content of dried mango slices (Cv. Apple and Kent). In: Advances of science and technology. Cham, Switzerland: Springer; 2022:97–109 pp.
2. Misra S, Pandey P, Dalbhagat CG, Mishra HN. Emerging technologies and coating materials for improved probiotication in food products: a review. Food Bioprocess Technol 2022;15:998–1039.
3. Ai Z, Zhu G, Zheng Z, Xiao H, Mowafy S, Liu Y. Successive two-stage hot air-drying with humidity control combined radio frequency drying improving drying efficiency and nutritional quality of amomi fructus. Food Bioprocess Technol 2023;16:149–66.
4. Ancos BD, Sanchez MD, Zacarias L, Rodrigo MJ, Sáyago Ayerdí S, Blancas Benítez FJ, et al. Effects of two different drying methods (freeze-drying and hot air-drying) on the phenolic and carotenoid profile of 'Ataulfo' mango by-products. J Food Meas Char 2018;12: 2145–57.
5. Shende D, Datta AK. Optimization study for refractance window drying process of langra variety mango. J Food Sci Technol 2019;57:683–92.
6. Koubala BB, Kansci G, Garnier G, Thibault G, Ralet M. Physicochemical properties of dietary fibres prepared from ambarella (Spondias cytherea) and mango (Mangifera indica) peels. Food Bioprocess Technol 2013;6:591–7.
7. Kumar PS, Sagar VR. Drying kinetics and physico-chemical characteristics of osmo-dehydrated mango, guava and aonla under different drying conditions. J Food Sci Technol 2014;51:1540–6.
8. Ridder D, Kroese F, Evers C, Adriaanse M, Gillebaart T. Healthy diet: health impact, prevalence, correlates, and interventions. Psychol Health 2017;32:907–41.
9. Husen R, Andou Y, Ismail A, Shirai Y, Hassan MA. Enhanced polyphenol content and antioxidant capacity in the edible portion of avocado dried with superheated-steam. Int J Adv Res 2014;2:241–8.
10. Husen C, Chiewchan N, Devahastin S. Thermal resistance of salmonella enterica serovar anatum on cabbage surfaces during drying: effects of drying methods and conditions. Int J Food Microbiol 2011;147:127–33.
11. Ramachandran RP, Akbarzadeh M, Paliwal J, Cenkowski S. Computational fluid dynamics in drying process modelling-a technical review. Food Bioprocess Technol 2018;11:271–92.
12. Mujumdar AS, Law CL. Drying technology: trends and applications in postharvest processing. Food Bioprocess Technol 2010;3:843–52.
13. Liu JB, Zang LT, Xu Q, Wang RF, Li ZY. Drying of soy sauce residue in superheated steam at atmospheric pressure. Dry Technol 2017;35: 1656–63.
14. Wang J, Xu Q, Liu J, Zheng S, Wang R, Li Z. Drying of pineapple slices using combined low pressure superheated steam and vacuum drying. Int J Food Eng 2021;17:865–75.
15. Schoeman L, Manley M. Oven and Forced Convection Continuous Tumble (FCCT) roasting: effect on physicochemical, structural and functional properties of wheat grain. Food Bioprocess Technol 2019;12: 166–82.
16. Brar NK, Ramachandran RP, Cenkowski S, Paliwal J. Effect of superheated steam- and hot air-assisted processing on functional and nutritional properties of yellow peas. Food Bioprocess Technol 2021;14: 1684–99.
17. Zhong Y, Zhang Y, Liu X, Liu C, Wu J, Huang H, et al. Structural characteristics of cooked black rice influenced by different stabilization treatments and their effect mechanism on the in vitro digestibility. Food Bioprocess Technol 2022;16:897–908.
18. Park HW, Balasubramaniam VM, Snyder AB, Sekhar JA. Influence of superheated steam temperature and moisture exchange on the inactivation of Geobacillus stearothermophilus spores in wheat flour-coated surfaces. Food Bioprocess Technol 2022;15:1550–62.
19. Erkinbaev C, Ramachandran RP, Cenkowski S, Paliwal J. A comparative study on the effect of superheated steam and hot air drying on microstructure of distillers' spent grain pellets using X-ray micro-computed tomography. J Food Eng 2019;241:127–35.
20. Pongmalai P, Devahastin S. Profiles of prebiotic fructooligosaccharides, inulin and sugars as well as physicochemical properties of banana and its snacks as affected by ripening stage and applied drying methods. Dry Technol 2020;38:724–34.
21. Mariia S, Wawrzyniak P, Meng WW. Superheated steam spray drying as an energy-saving drying technique: a review. Energies 2022;15:1–22.
22. Liu JB, Xue J, Xu Q, Shi YP, Wu L, Li ZY. Drying kinetics and quality attributes of white radish in low pressure superheated steam. Int J Food Eng 2017;13:1–13.
23. Luo GY, Song CF, Pu HJ, Li ZF, Xu WX, Raghayan GSV, et al. Optimization of the microwave drying process for potato chips based on the measurement of dielectric properties. Dry Technol 2019;37:1329–39.
24. Wang T, Xue YJ, Hao R, Hou HB, Liu JX, Li JP. Mechanism investigations into the effect of rice husk and wood sawdust conditioning on sewage sludge thermal drying. J Environ Manag 2019;239:316–23.
25. Toma RB, Leung HK. Determination of reducing sugars in French fried potatoes by 3,5-dinitrosalicylic acid. Food Chem 1987;23:29–33.
26. Zhuang JL, Yu Y, Yang LL, Zhang JH, Jin Y, Feng B. Identification of zeaxanthin dipalmitate by high performance liquid chromatography. Food Industry 2020;41:306–10.
27. Malaikritsanachalee P, Choosri W, Choosri T. Study on intermittent low-pressure superheated steam drying: effect on drying kinetics and quality changes in ripe mango slices. J Food Process Preserv 2020;44: e14669.
28. Cai JR, Lu Y, Bai JW, Li S, Hongwei X. Three-dimensional imaging of morphological changes of potato slices during drying. Trans Chin Soc Agric Eng 2019;35:278–84.
29. Goncalves EM, Pinheiro J, Abreu M, Brandao TRS, Silva CLM. Carrot (Daucus carota L.) peroxidase inactivation, phenolic content and physical changes kinetics due to blanching. J Food Eng 2010;97: 574–81.

30. Seremet L, Botez E, Nistor OV, Andronoiu DG, Mocanu GD. Effect of different drying methods on moisture ratio and rehydration of pumpkin slices. Food Chem 2016;195:104–9.
31. Li ZY, Liu JB, Xu Q, Shi YP. Study on inversion temperature in low pressure superheated steam drying of green turnip slice. Trans Chin Soc Agric Eng 2018;34:279–86.
32. Wang RF, Wang JC, Zhao DH. Drying of banana using combined low-pressure superheated steam and vacuum drying. Trans Chin Soc Agric Mach 2022;53:392–9.
33. Devahastin S, Suvarnakuta P, Soponronnarit S, Mujumdar AS. A comparative study of low-pressure superheated steam and vacuum drying of a heat-sensitive material. Dry Technol 2004;22: 1845–67.
34. Liu SP, Zeng E, Wu QR, Wang GM, Zhang XK, Wei H. Research progress of low-pressure superheated steam drying heat-sensitive materials. Food Industry 2017;38:204–7.
35. Sittiritkawin P, Achariya S, Achariyaviriya A, Namsanguan K. Investigation of drying pumpkin slices by low-pressure superheated steam. Int Agric Eng J 2017;26:200–12.
36. Nimmol C, Devahastin S, Swasdisevi T, Soponronnarit S. Drying of banana slices using combined low-pressure superheated steam and far-infrared radiation. J Food Eng 2007;81:624–33.
37. Matsuura R. Verification of healthy effects with superheated steam technology. Japan J Food Eng 2009;10:77–8.
38. Suvarnakuta P, Chaweerungrat C, Devahastin S. Effects of drying methods on assay and antioxidant activity of xanthones in mangosteen rind. Food Chem 2011;125:240–7.
39. Liu JB, Xu Q, Shi Y, Wang RF, Li ZY. Influence of steam condensation on vitamin C retention in green turnip undergoing low pressure superheated steam drying. J Food Process Eng 2018;41:e12898.
40. Messai S, Sghaier J, Chrusciel L, El Ganaoui, M, Gabsi, S. Low-pressure superheated steam drying vacuum drying of a porous media and the inversion temperature. Dry Technol 2015;33:111–19.
41. Almeida RLJ, Santos NC, Ferreira ILS, Pedro MS, Morais JRF, de Oliveira AP, et al. Impact of treatment with superheated steam on the structural, thermal, and functional characteristics of quinoa starch. Starch 2023;75(11–12):23000101.
42. Santos JG, Perez RM, Sotia AC, Olano A, Montill A, Villamiel M. Impact of processing conditions on the kinetic of vitamin C degradation and 2-furoylmethyl amino acid formation in dried straw-berries. Food Chem 2014;153:164–70.
43. Herbig AL, Renard CMGC. Factors that impact the stability of vitamin C at intermediate temperatures in a food matrix. Food Chem 2017;220: 444–51.
44. Phothisoot T, Gavahian M, Lin J. Sustainable superheated steam drying of unripe banana (Musa acuminata cv. Hom Thong): effects on resistant starch and physicochemical–functional properties. Starch 2023;23000101. https://doi.org/10.1002/star.202300101. Submitted for publication.
45. Cheevitsopon E, Noomhorm A. Effects of superheated steam fluidized bed drying on the quality of parboiled germinated brown rice. J Food Process Preserv 2015;39:349–56.
46. Head DS, Cenkowski S, Arntfield S, Henderson K. Superheated steam processing of oat groats. LWT – Food Sci Technol 2010;43:690–4.